COMPARATIVE INVESTIGATION OF RADIATION RESISTANCE OF A NUMBER OF THE TOKAMAK PLASMA FACING CERAMIC MATERIALS BY MEANS OF PLASMA FOCUS DEVICES

E.V. Demina[1], V.A. Gribkov[1,2,3], A.V. Dubrovsky[1], V.N. Pimenov[1], S.A. Maslyaev[1,2], V.A. Ermishkin[1], M. Chernyshova[2], R.A. Miklaszewski[2], M. Paduch[2], M. Scholz[2], E. Zielińska[2], R. Gaffka[3], M. Gryaznevich[3], M. Sadowski[4], E. Skladnic-Sadowska[4], C. Tuniz[5]

[1] *A.A. Baikov Institute of Metallurgy and Material Science, 119 991 Moscow, Russian Federation*
[2] *Institute of Plasma Physics and Laser Microfusion, 01-497 Warsaw, Poland*
[3] *EUROATOM/CCFE Fusion Association, Culhan Science Centre, Abingdon, United Kingdom*
[4] *A Soltan Institute for Nuclear Studies, 05-400 Otwock-Swierk n.Warsaw, Poland*
[5] *The Abdus Salan International Centre for Theoretical Physics, 34014 Trieste, Italy*

I. INTRODUCTION

Our activity has been concentrated in a study of ceramic material. Various types of ceramics are now more and more widely used in the mainstream nuclear fusion facilities because of their high insulation properties, elevated heat and radiation resistance compared with other commonly employed isolators (e.g. plastics).
Three types of ceramic materials were studied experimentally:

The carbon-fiber composites CFC/SiC (these materials show considerable promise to be applied partly for the divertor manufacture of tokamak);

Boron Nitride (BN) and alumina (Al_2O_3) - these materials are a prospective to be used as a cover of the antenna coils placed inside the discharge chamber of the spherical tokamak named MAST).

Experiments were carried out on PF-1000 Plasma-Focus device.

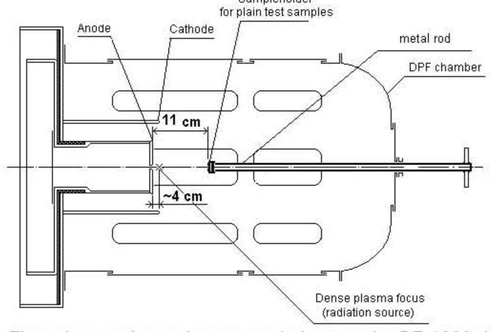

Fig.1 The scheme of experiments carried out on the PF-1000 device

II. PLASMA AND BEAM DYNAMICS

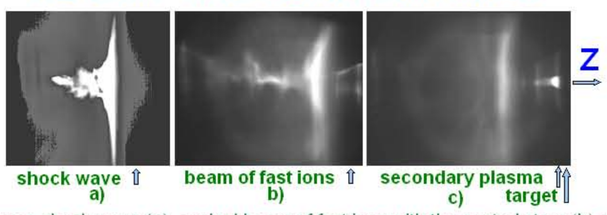

Fig. 2 Plasma shock wave (a), conical beam of fast ions with the central stem (b) and secondary (ablation) plasma near the target's surface – images taken by self-luminescence of the objects with the exposure time 1 ns

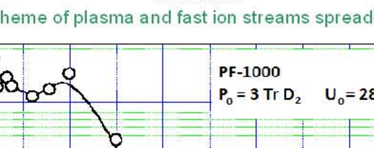

Fig. 3 Scheme of plasma and fast ion streams spreading into space

Fig. 4 Dynamics of temperature and density of secondary plasma produced on the surface of specimens by streams of hot plasma and beam of fast ions

III. STUDIES OF CARBON-FIBER COMPOSITS

a) **Investigated materials**

The investigated specimens were made of a CFC/SiC composite material consisted of carbon fibers reinforced by particles of silicium carbide with 8 and 40 %vol., i.e. CFC-8SiC and CFC-40SiC, respectively. The samples were manufactured as rectangular prisms of dimensions equal to (1×1×0.8) cm^3.

b) **Irradiation conditions**

The specimens were placed inside the chambers of the applied DPF devices at various distances from the anode outlets (in the PF-1000 facility – at distances from 11 cm to 54 cm), but near the Z-axis, where they were as subjects of the irradiation by hot plasma streams and fast ions beams

Table I. Irradiation conditions

Material	Distance from the anode L, cm	Number of the irradiation pulses	Power flux density q, 10^8 W/cm^2	Duration of pulses (powerful stage + discharge decay), μs
CFC-8SiC	12	5	10	0.2 + 100
CFC-40SiC	12	5	10	

The results of an optical microscopy

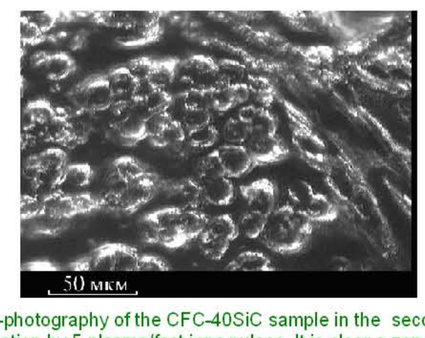

Fig. 5 Micro-photography of the CFC-40SiC sample in the secondary electrons after irradiation by 5 plasma/fast ions pulses. It is clear a zone where fibers were oriented mainly perpendicular to the sample surface

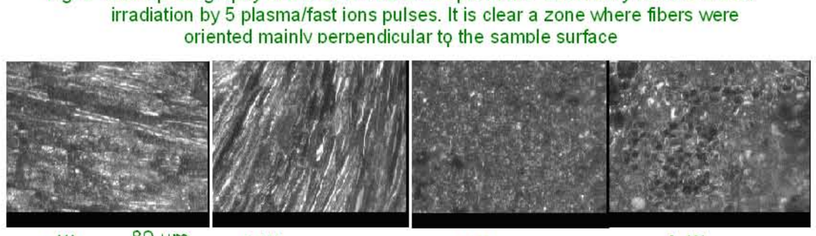

Fig. 6 Micro-photography of some regions of the CFC-8SiC specimens (1 – with fibers parallel to the irradiation plane, 2 – with fibers perpendicular to this plane): (a) - for the virgin sample, (b) – for that irradiated by 5 pulses of deuterium plasma.

It was observed that the fibers of the orientation perpendicular to the irradiation surface lost material mainly from their crosscut ends. It was also found that the strongest erosion took place in central parts of the crosscut ends of the fibers, and it produced noticeable depressions in these regions. A similar picture was obtained for the CFC-40SiC material.

Results of structure-phase analysis

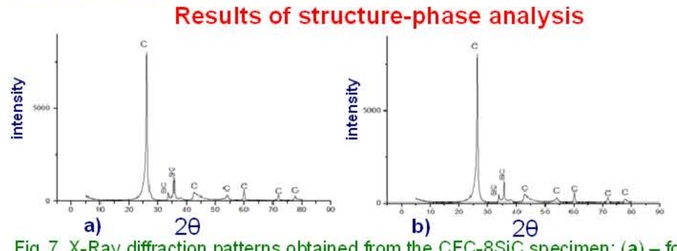

Fig.7 X-Ray diffraction patterns obtained from the CFC-8SiC specimen: (**a**) – for the virgin state, and (**b**) after irradiation by 5 pulses of deuterium plasma at $q = 10^9$ W/cm^2

The result shows a good structure stability of the investigated material against the irradiation in the tough regime.

Study of the erosion

Table II Thickness of the CFC/SiC layer evaporated during the irradiation by deuterium plasma

Material	Power flux density, q W/cm^2	Number of pulses, N	Thickness of the layer evaporated for a single pulse, d μm
CFC – 8SiC	10^9	5	2.646
CFC – 40SiC	10^9	5	1.948

Table II presents some results of estimation of the thickness d of the evaporated layer of samples for the case when fibers of the CFC material are directed mainly in parallel to the vector of the irradiating stream.
The evaporation process at q = 10^9 W/cm^2 is quite intensive: thickness of the layer evaporated for a single pulse is of 2 μm or more. In the case, when fibers are oriented perpendicular to the stream thickness falls about 2 times in value.

Distribution of elements

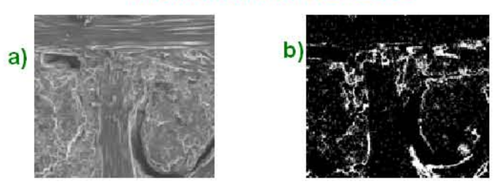

Fig. 8 Photographs from the scanning of the CFC-8SiC sample surface after five pulses in the secondary electrons (a) and in the characteristic x-rays of Si (b)

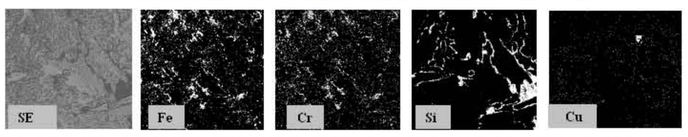

Fig. 9 Photographs from the scanning of the CFC-8SiC sample surface after irradiation by 5 plasma/fast ions pulses in the secondary electrons and in characteristic X-Rays of Fe, Cr, Si and Cu.

We were observed the processes of evaporation and sputtering of the surface layers by plasma-ion streams, as well as the deposition of some elements originating from constructional materials of the PF-1000 facility. It is clear that different elements implanted into the volume of SL interacted with each other and with the substrate material producing compounds of the type of carbides and intermetallic phases. Such compounds may influence upon diffusion penetrability of deuterium ions through the matrix of the CFC/SiC composite.

IV. STUDIES OF ALUMINA AND BORON

Irradiation tests of BN and Al_2O_3 ceramics

The irradiation tests were carried out on the PF-1000 device. The specimens were placed at the distances of 15 cm or 30 cm from the PF-1000 electrodes outlet and they were exposed to 1 - 8 shots. The interaction period of so-called "powerful phase" of the PF-1000 discharge was about 0.2 - 2 μs for plasma streams and 0.2 - 0.6 μs for the fast ions beams, while the whole period of plasma action upon the specimens was about 100 μs. The positions of the samples were chosen to achieve conditions of three different types: 1. Below the material melting point; 2. Corresponding to the melting point; and 3. High above the melting point.

Fig. 10 A picture of the specimens' fixation BN on the top left and Al_2O_3 on the bottom; see the semicircular dark spot on it – the result of irradiation by the axial beam of fast ions

Fig.11 Photos of the specimens of ceramics of both types: plates are the aluminum slices covered with the Al_2O_3, cube – NB; (a) – after the irradiation at a distance 30 cm by a single pulse, (b) – same distance but 4 pulses, (c) – 15 cm and 8 pulses

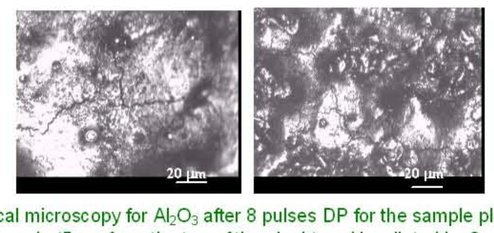

Fig. 12 Optical microscopy for Al_2O_3 after 8 pulses DP for the sample placed in 15 cm from the DPF anode (5 cm from the top of the pinch) and irradiated by 8 plasma-ion pulses

It appears that after 8 pulses of fast ion stream having power flux density about 10^{10} W/cm^2 and of plasma stream having power flux density 10^{8-9} W/cm^2 ceramic layer was almost completely evaporated and pure melted aluminum (white color in the picture) and cracks become apparent.

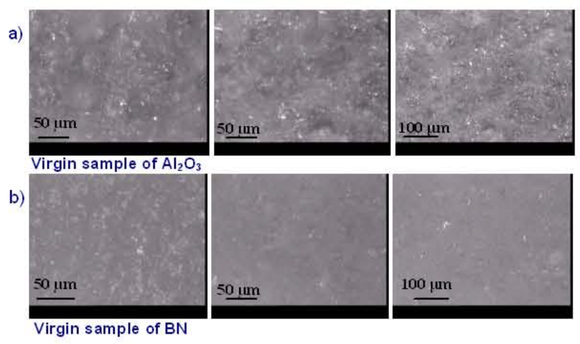

Fig. 13 Central parts of the specimens of Al_2O_3 (**a**) and BN (**b**), after a single-pulse action of deuterium plasma and beam of fast ions ($q \sim 10^8$ W/cm^2 for plasma stream and 10^9 for the beam of fast ions)

One can see that the character of the surface of both samples after irradiation is approximately the same

Results of the sample's evaporating

Table III Thickness of the evaporated Al_2O_3

No of a sample	Power flux density, q W/cm^2	Mass before irradiation, g	Mass after irradiation, g	Mass change, g	Distance from the anode, cm	Number of pulses	Thickness of the evaporated layer, μm
1	10^{10}	9.1339	9.0520	81.9	15	8	200
2	10^9	8.9270	8.9161	10.9	30	4	27.4
3	10^9	5.3029	5.3013	1.6	30	1	4

Table IV Thickness of the evaporated BN

No. of a sample	Power flux density, q W/cm^2	Mass before irradiation, g	Mass after irradiation, g	Mass change, g	Distance from the anode, cm	Number of pulses	Thickness of the evaporated layer, μm
1	10^8	2.6503	2.6456	4.7	30	4	20
2	10^8	2.6434	2.6419	1.5	30	1	6.4

One can see from Tables III and IV that the thicknesses of evaporated layers of both materials in the regime without melting are about the same value. However, since the power flux density irradiating BN is an order of magnitude lower than in the other case, the intensity of its evaporation is significantly higher than in Al_2O_3 case.

X-Ray structure (phase) analysis

Al_2O_3/Al-substrate; specimen No.1 (15 cm, 8 pulses, melting)

Table V Approximate phases content of specimen No. 1

Phase	Volumetric %	
	Central part	Sample's edge
Al	91, 74	92, 59
Al_2O_3	–	0, 93
Compositions of Al with Cu and Fe	8, 26	6, 48

The surface layer (SL) of the sample was melted more profoundly in its centre and after recrystallization a low-grain structure was created along the grad T.

Specimen Al_2O_3 №2 (30 cm, 4 pulses)

The character of the lines in DP is about the same as in the virgin sample but there are some differences in intensities.

Table VI Approximate phases content of specimen No. 2

Phase	Volumetric %	
	Central part	Sample's edge
Al	93, 46	93, 46
Al_2O_3	2, 79	0, 93
Compositions of Al with Cu and Fe	3, 75	5, 61

One may see that concentration of Al_2O_3 in the central part of the sample is much higher than that at its periphery.

Sample Al_2O_3 No. 3 (30 cm, 1 pulse)

Table V Approximate phases content of specimen No. 3

Phase	Volumetric %	
	Central part	Sample's edge
Al	94, 02	94, 02
Al_2O_3	3, 16	3, 76
Compositions of Al with Cu and Fe	2, 82	2, 82

One can see that in that case the concentration of Al_2O_3 in the central part (where the dark spot resulted from the ion beams action, see Fig. 10 (a), zone 2) was considerable lower than that outside of this region (i.e. in zone 1).

One may see that concentration of Al_2O_3 in the central part is higher than that in specimens No1 and No2.

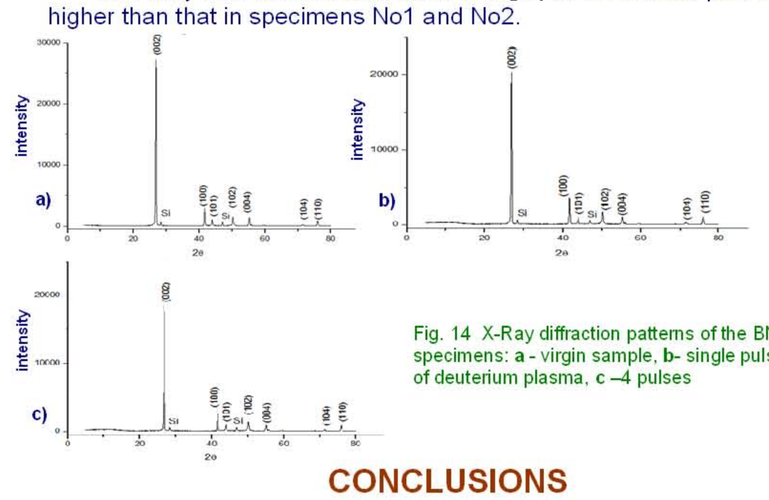

Fig. 14 X-Ray diffraction patterns of the BN specimens: **a** - virgin sample, **b**- single pulse of deuterium plasma, **c** –4 pulses

CONCLUSIONS

1. Characteristic features of material damage based on a carbon-fiber composite (CFC) with additions of SiC of 8 and 40 vol.% were studied. A good structural stability of the CFC/SiC material to high-energy pulsed ion beams and plasma streams in the hard mode of irradiation was shown. It was also found that at q = 10^9 W/cm^2 an erosion of the surface layer is mainly associated with the processes of sputtering and evaporation of the material. Degree of erosion depends on orientation of fibers in relation to the direction of the streams and on the percentage of the SiC dopant. This process decreases when carbon fibers of the composite are oriented normally to the vectors of the incident energy flux.
2. After eight pulses with 10^{10}W/cm^2, the Al_2O_3 coating was almost completely evaporated, and melted Al appeared at the surface showing many cracks; in contrast, four pulses of 10^8–10^9 W/cm^2 did not show noticeable cracks on these and on the BN samples.
3. A direct comparison of Al_2O_3 and BN materials was made after a single 10^8–10^9W/cm^2 pulse, and it appeared that although surface structure changes were higher for Al_2O_3, the evaporation of BN was about two times higher than that of Al_2O_3. This was so despite the fact that the BN sample was not at the ion stream axis and obtained an order of magnitude lower flux.
4. The X-ray phase analysis of the exposed samples showed no evidence of the Al_2O_3 cracking even at the highest loads (in spite of some melting), which suggests that the insulation properties of Al_2O_3 did not decline at least below melting point (although this result should be checked by direct measurements of the layer resistance after the irradiation).